Indian Journal of Geo Marine Sciences
Vol. 51 (10), October 2022, pp. 801-810
DOI: 10.56042/ijms.v51i10.2929

Microenergy harvester for remote ocean buoys using piezoelectric sensors coupled with superballs

J M Hann*[,a], B V Mudgal[a] & T P S Jinoj[b]

[a]Centre for Water Resources, CEG Campus, Anna University, Chennai – 600 025, India
[b]National Centre for Coastal Research, NIOT Campus, Velachery - Tambaram Main Rd, Pallikaranai, Chennai – 600 100, India
*[E-mail: mahijahann@gmail.com]

Received 23 September 2022; revised 30 October 2022

Wave energy is a renewable resource with high energy potential. This research work proposes a low power piezoelectric energy harvesting system based on the heave motion of ocean buoys. This Piezoelectric Energy Harvester (PEH) is composed of piezoelectric diaphragms coupled with superballs to enhance the output of the piezoelectric sensor. The PEH setup is designed within a floating buoy and tested in a wave flume by varying the frequency of regular waves. The heaving of the buoy causes the superball to oscillate and impact upon the piezo diaphragms thereby producing power. This output is then processed using appropriate AC to DC converter and booster circuits. The single-axis sensor-diaphragm responses under regular wave conditions with varying wave heights were analyzed. A rms voltage of about 2.56 V was generated for a wave height of 0.21 m and wave period of 1.2 s. The wave flume experimental results show that the maximum harvested power was about 80 mW by the entire piezo sensor diaphragm setup for the wave height range of 0.06 m to 0.21 m and wave period of 1.22 s to 2.13 s. Using the same technique in the ocean buoys of diameter 0.9 m in the swell wave conditions between 0.5 to 3.5 m significant wave height, the system can generate maximum voltage of up to 16 V using 28 numbers of superballs with sensors arranged in parallel/series combinational power circuits. This harvesting technique will be very much useful for coastal & offshore buoys to harvest power in a hybrid approach during the failure in solar battery charging during monsoon and unfavorable weathers.

[**Keywords**: Energy harvesting, Microgenerator, Microprocessor, Piezoelectric diaphragm, Superball, Waveflume]

Introduction

During the past few decades there have been lot of researches related to renewable energy, especially with respect to the wave energy converters from the ocean[1-4] due to climate change[5], natural disasters[6], blue energy harvesting[7] and coral health monitoring[8]. A wide range of instruments and sensors are deployed in the ocean to measure the ocean's physical, chemical and meteorological parameters. Since there is no possibility for grid supply in these remote locations, there is a demand for self-powered devices. Most of the systems currently available are battery powered. But the life of the battery is considerably reduced in the harsh oceanic environment as they suffer from inherent maintenance and frequent recharging. These prompted researchers to look for alternative energy sources to power up the onboard sensors whose operating voltages and current requirements are considerably less[9].

One of the earliest concepts of self-powered devices was proposed in 2006 by Wang & Song[10]. Many systems currently make use of solar panels or solar cells to power up the sensors. This form of energy is available only under appropriate ambient conditions and is not available throughout the year. The cost of installation and maintenance is also very high and they are bulky hence not suitable for all areas. The power density of the ocean waves is higher when compared to wind and solar. The power density of photovoltaic cell is 1 kW/m^2 at peak solar isolation, for wind it is 1 kW/m^2 at 12 m/s [General Electric (GE) 1.5-MW machine] but, for wave energy it is 25 kW/m at San Francisco, average annual power flux[11]. Hence, lots of researches are focusing on wave energy converters.

Floating type wave energy harvesters have proven to be fairly good for harnessing wave energy. The first commercial floating design was patented by the Finnish company Wello[12]. It consists of a rotating pendulum attached to a shaft inside a buoy to generate electricity. The shaft rotates as the pendulum rotates and this mechanical energy is then converted to electrical power. Other forms of ocean wave energy converters are the overtopping device wave dragon, Archimedes wave, oscillating water columns and the hinged contour devices as the Pelamis[13]. Amongst

these, the heaving point absorbing wave energy converters have a simpler architecture and they convert the wave energy directly, so its conversion efficiency is high. It is also suitable for waters of different depths because of its mooring mechanism. Lot of researches focusing on combining different renewable energy generation has come up in the recent years. Taylor *et al*.[14], proposed a piezoelectric eel to harvest energy from the flow of the oceans. A hybrid generator combining both triboelectric and piezoelectric harvesters was suggested by Li *et al*.[15].

Piezoelectric generators are based on the piezoelectric effect discovered by Pierre & Jacques Curie; when mechanical pressure is applied to any opposite faces of the piezoelectric material there is charge production along the other two faces of the material[16]. The amount of power generated using piezoelectric harvesters is generally in the milli watt range. This is attributed to the fact that the piezoelectric ceramics can accept large stresses but, their strains are very small. Most of the onboard sensors have the power requirement in the mW or l W range and they depend upon compact power sources which could be easily mounted onboard thereby making piezoelectric harvesters versatile for low power applications. Wang *et al*.[17], show that using a piezoelectric circular array in series connection increases the output energy compared to a single diaphragm. The amount of electric energy produced from the piezoelectric harvester circuit will be directly proportional to the frequency and stress by resonant vibration that hits on the piezoelectric sensor. Frequency is the major factor to be considered for maximizing the output of the PEH as the maximum power is generated at the resonance frequency of the chosen piezoelectric material.

This research work is focused on developing a PEH which can be incorporated inside the cavity of the buoys. The Piezo diaphragm is triggered by the impact of the superballs on it thereby producing power. The received power is converted and stored in the battery which can be used to power up the onboard sensors.

Materials and Methods

The PEH consists of two parts: the mechanical part, for the generation of electrical energy and the support system that consists of electrical parts for the conversion and storage of the generated energy along with a data logger. The piezoelectric sensors, superball for piezo sensor vibration and accelerometer/gyroscope sensors are constituents of the mechanical part whereas; the rectifier, booster circuits, microcontroller & processor, and storage system constitute the electrical part. The schematic representation of Piezoelectric Energy Harvester (PEH) system is given in Figure 1. The AC to DC converter circuit used for this study achieved 91 % efficiency.

The piezoelectric sensor is made of piezoelectric ceramic and when stress is applied to the transducer, the ions in the material move towards one of the conducting surface while moving away from the other. This results in the generation of charge which can be stored in rechargeable batteries or capacitors. The polarity of the produced charge depends upon the direction of the applied stress.

In the longitudinal effect the charge generated is given by:

$$Q = F * d \quad \ldots (1)$$

Where, F is the applied force, and d is the piezoelectric coefficient of the crystal. Piezoelectric

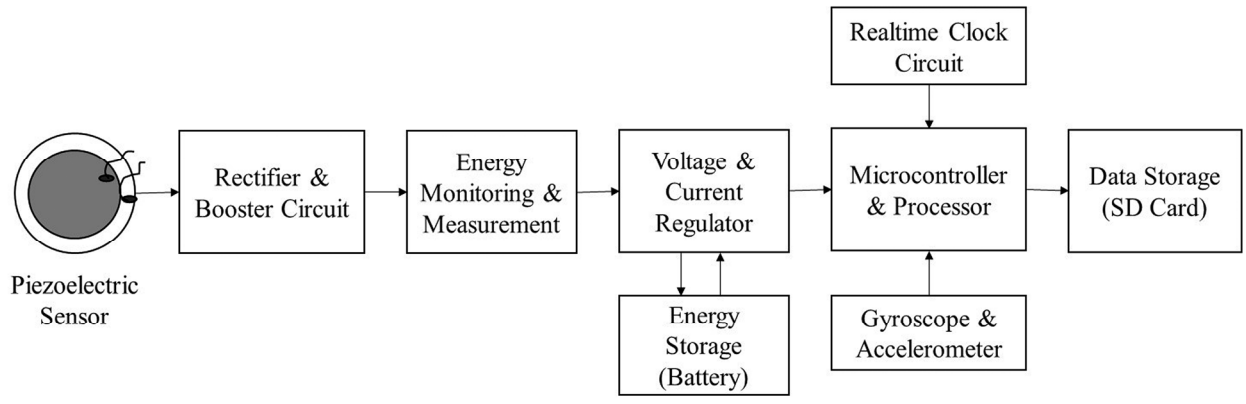

Fig. 1 — Schematic representation of Piezoelectric Energy Harvester (PEH) system

coefficient d of quartz crystal is around 3×10^{-10} m/V.

Four piezoelectric diaphragms from Murata Electronics North America, Inc. (Smyrna, GA, USA) were used in the experiment. Each diaphragm has a thickness of 0.92 mm with plate diameter of 34 mm, element diameter 24 mm and the plate material is brass resonant. The impulse response of the piezo sensor is 5 µs and the efficient frequency of operation is around 6 kHz. The diaphragms are oriented in a bottom inside manner so that the impact of the ball is upon the brass plates.

Superballs made of polybutadiene, a synthetic rubber material which makes the ball bounce thereby resulting in resonant vibration is used. This is because the super ball made of synthetic rubber material rebounds with a higher velocity which ensures the continuous functioning of the harvester thereby increasing the power output. The coefficient of restitution of the super ball is higher than that of steel or iron ball. When these balls are dropped, they convert the potential energy into kinetic energy which enables them to rebound with the fraction of their original force this is due to the high coefficient of restitution. Coefficient of Restitution (COR) is the measure of the velocity of return of the object dropped; it shows the amount of energy maintained inside the object after striking against the surface[18]. For an object bouncing off a stationary surface the coefficient of restitution is given as:

$$C_r = \frac{v}{u} = \sqrt{\frac{h_2}{h_1}} \quad \ldots (2)$$

Where, u and v are the relative velocity before and after collision. The values of the COR varies from 0 – 1. The four balls used in this experiment have a mass of 0.5 g, diameter of 2.2 cm with measured u and v as 50.47 mm/s and 53.92 mm/s, respectively. From this the coefficient of restitution is calculated to be around 0.93.

When the ball hits the surface of the piezo sensor it recoils and vibrates which in turn triggers the production of energy. The energy equation for the super ball hitting the piezo sensor is based on mass m, height h of free fall and the velocity v upon the impact[19]. The energy equation can be written as:

$$mgh = \frac{1}{2}mv^2 \quad \ldots (3)$$

Where, m is mass of the ball, g is the acceleration of gravity, h is the height, and v is the velocity of impact

$$v = \sqrt{2gh} \quad \ldots (4)$$

When the ball hits the piezo sensor with velocity v and travels the height h_1, then the total impact force from the sensor is calculated by the equation:

$$F = \frac{E_k}{h_1} = \frac{mv^2}{2h_1} \quad \ldots (5)$$

Where, F is the impact force, and E_k is the kinetic energy.

The velocity v of super ball changes with the wave frequency, wave height of the PEH harvester system in ocean environment. The impact force can be modified further by changing the mass m of the ball. The mass m of the ball and the resonant vibration/hitting of ball on the piezo sensor are inversely proportional. The superball is allowed to move freely inside the PVC tube and it impacts the piezoelectric diaphragm at both the ends. The Piezo-diaphragm gets excitation using the super ball made of polybutadiene, a synthetic rubber material and efficiency of the electrical energy will be high during vertical rebounding.

The efficient energy harvesting circuit has a capacitor (C) and the diode for rectification. In the capacitor, the maximum charges occur during the vibration of piezo sensor. Rectifier circuit has been used for converting the generated low power AC to DC. The regulator circuit rectifies the ripples from the input DC power to the constant DC voltage which can be connected to storage devices. The regulator component is implemented by suitable voltage regulator IC along with current limiting resistor and capacitors.

The setup makes use of an ATMega 2560 microcontroller which accommodate real-time counter with different oscillator, programmable watchdog timer with individual on-chip oscillator, on-chip analog comparator and an interrupt and wake-up on pin charge. The microcontroller connected with accelerometer senses the inertial movements by measuring the angular or linear acceleration. The non-gravitational acceleration generated by forces of motion in the water column by waves or currents other than gravity or inertial forces can be measured and the accelerometer is enabled with offsets in the measurements due to local gravity. In this experimental study, the waves generated in the wave flume excite the piezo sensor using superball due to the motion in floating PEH buoy setup. The MEMS accelerometer with the microcontroller mounted in

the PEH buoy measures the acceleration, heave, pitch and roll. MPU6050 sensor 6-axis motion tracking module is used for the purpose of accelerometer and gyroscope with MEMS technology. The MEMS accelerometer is configured with 10 Hz sampling frequency for the efficient data collection and processing. The accuracy of the 3-axis gyroscope and accelerometer used in this experiment is 1 to 2 degree heading accuracy with the max data rate 160 Hz. The module combines a 3-axis gyroscope, accelerometer and a digital motion processor having I^2C bus interface to interconnect with microcontrollers. The auxiliary I^2C bus is enabled to link sensor devices like pressure sensor, 3-axis magnetometer, etc. The I^2C-bus is the most efficient interface to connect 3-axis gyroscope and accelerometer sensor and the microcontroller with Real-Time Clock (RTC). The 3-axis gyroscope and accelerometer are used to detect rotational velocity, angle of tilt or inclination along the X, Y, Z axes. This sensor has several registers to control and configure its approach of operation. The gyroscope and accelerometer sensor data module comprises of 16-bit raw data in 2's complement form. The four piezoelectric diaphragms along with the four superballs for providing impact are arranged in a cubical box as shown in Figure 2.

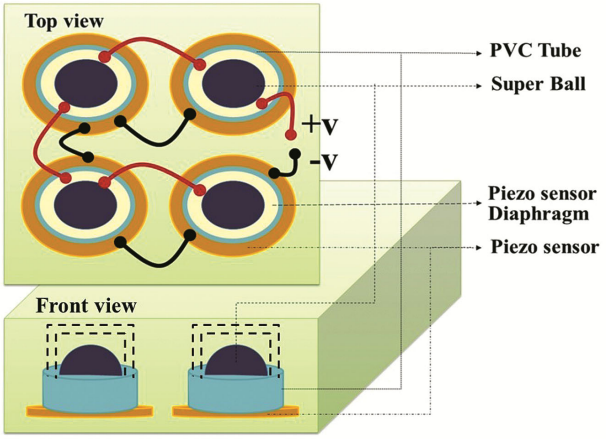

Fig. 2 — Sketch of the Piezoelectric Energy Harvester (PEH)

Wave flume experimentation setup

The ocean waves can be characterized as linear, nonlinear and random. In this study regular waves are generated in a wave flume. The wave flume is an excellent tool for the analysis of wave energy converters as it helps to simulate and study real wave action in the laboratory. The wave flume is divided into three areas the wave generating area, the test area and the beach profile which helps to dissipate the wave. The flume is about 30 m in length, it has a height of 1 m and the width of the flume is about 1 m. The beach profile is made up of a slope 1:8 consisting stones roughly 20 cm in size. The wave generating area is enabled with wave paddle that is able to generate regular waves of frequency up to 1.5 KHz which is automated using the Labview software. Figure 3 shows the schematic sketch of the wave flume used.

The transducer unit is encased in an axisymmetric buoy and it is moored inside the wave flume as shown in Figure 4. Water is filled up to the 70 cm mark inside the flume. While the display unit along with the logger is placed outside the flume. The wave interaction in the flume sets the ball into motion which excites the piezo diaphragm and produces power. The six different excitation conditions were implemented in the wave flume by changing the wave shutter frequency from 30 to 60 Hz with a regular interval of 5 Hz for the duration of 10 min per selected frequency. The changes in the heave, pitch and roll with respect to varied wave excitation using wave generator is measured using the microcontroller. The accelerometer and gyroscope time series data was collected to calculate the heave, pitch, and roll using the data logger and onboard microcontroller and processor. The microcontroller board and the sensors consume less power and it is more reliable in

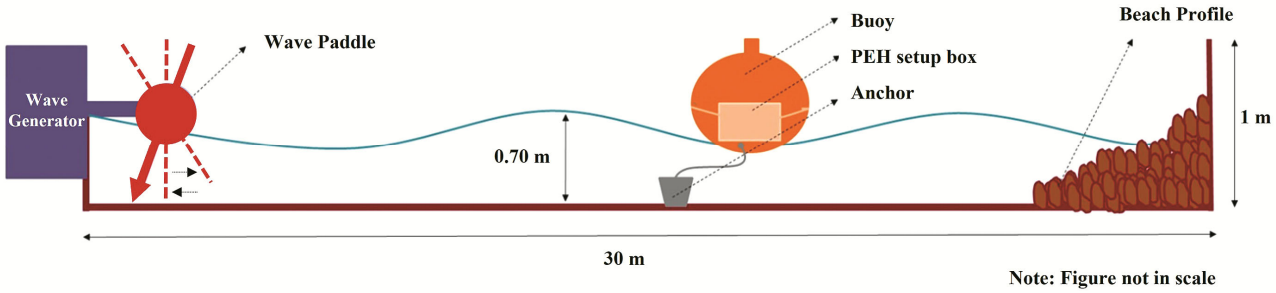

Fig. 3 — Sketch of flume (not to scale)

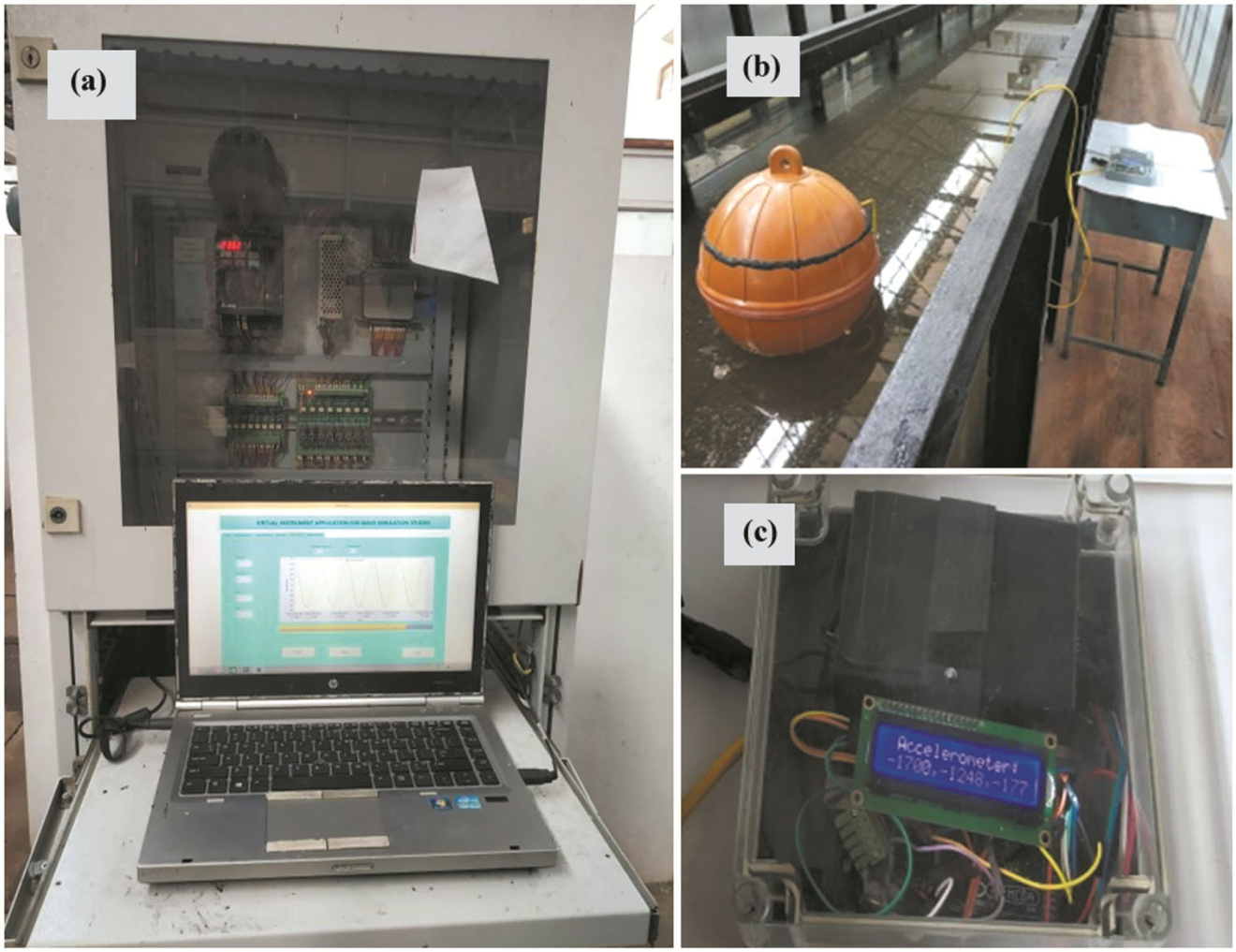

Fig. 4 — The PEH setup in the wave flume environment: (a) Wave generator hardware setup along with the Lab view software, (b) PEH buoy in the wave flume before the experiment, and (c) Data logger and microcontroller module of PEH system

providing accurate time series data after processing the datasets.

The six varied wave action with shutter frequency 60, 55, 50, 45, 40, and 35 Hz was generated in the wave flume to analyze the high- and low-level voltage generation using the PEH setup. The wave flume shutter frequency is automated within the frequency range of 35 to 60 Hz due to the limitations in wave flume physical features and design size. The Figure 5 shows the variations in the wave height (m) with respect to the varied wave period. The sampling frequency rate for the data collection is around 10 samples / second. The wave height, wave period and wavelength with respect to wave flume shutter frequency are given in Table 1. The wavelength is the distance between two crests or troughs and is found by solving the following equation[20,21].

$$\sigma^2 = gk \tanh(kd) \quad \ldots (6)$$

The angular wave frequency, σ is given as:

$$\sigma = \frac{2\pi}{T} \quad \ldots (7)$$

The wave number is given as:

$$k = \frac{2\pi}{L} \quad \ldots (8)$$

However, this is an implicit equation and it has to be solved numerically with the help of wave tables. The deep water approximation of wavelength L_0 can be obtained from:

$$L_0 = \frac{g}{2\pi}(T^2) \quad \ldots (9)$$

The gravitational constant, g is 9.81 and T represents the time period between crest and trough. For each L_0 value the $\frac{d}{L_0}$ value is calculated by using

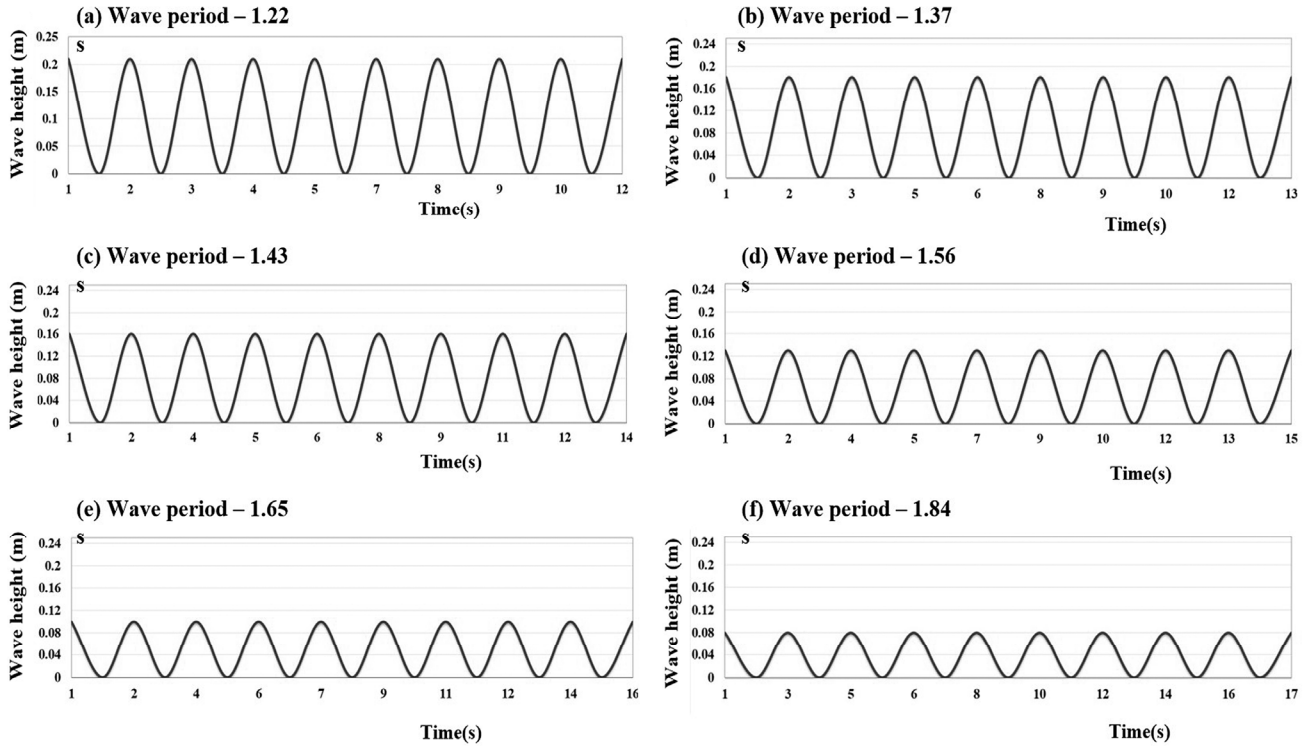

Fig. 5 — The variations in the wave height (m) with respect to the variations in wave period during different shutter frequencies (60 Hz, 55 Hz, 50 Hz, 45 Hz, 40 Hz & 35 Hz)

Table 1 — Wave height, wave period and wave length generated in the wave flume with varied shutter frequency along with the maximum voltage generated

S. No.	Shutter frequency (Hz)	Wave height (m)	Wave period (s)	Wavelength (m)	Maximum voltage (volt)
1	60	0.21	1.22	2.24	2.56
2	55	0.18	1.37	2.78	2.54
3	50	0.16	1.43	2.89	2.52
4	45	0.13	1.56	3.36	2.51
5	40	0.10	1.65	3.64	2.48
6	35	0.08	1.84	4.19	2.46
7	30	0.06	2.13	4.96	2.45

the water depth. Using the wave table the corresponding $\frac{d}{L}$ value is noted and from this the wavelength L is obtained. The depth of water in the flume is d = 0.7 m.

From the above calculations it is inferred that the waves make use of the linear airy wave theory as the wave height is infinitely small compared to the other wave parameters like wavelength and water depth. From Figure 5 and Table 1, it can be seen that the frequency of the waves increases as the wavelength decreases, thereby increasing the bounce of the super ball on the diaphragm and in turn increasing the power output. The output of PEH is connected with the resistor load of 10 KΩ and the corresponding voltage is recorded in microcontroller based data logger with the sampling interval of 10 µs.

Results and Discussion

The wave power and wave forces are theoretically calculated using the formulae given below. The wave energy flux per unit of wave-crest length is given as[22]:

$$P = \frac{\rho g^2}{64\pi} H_s^2 T_e \quad \ldots (10)$$

Where, ρ is the water density which is 1000 kg/m^3 for the fresh water used in the flume. H_s is the significant wave height, T_e is the wave energy period, and g is the acceleration due to gravity.

The heaving buoy is subjected to the forces namely: waves, gravitational, buoyancy and

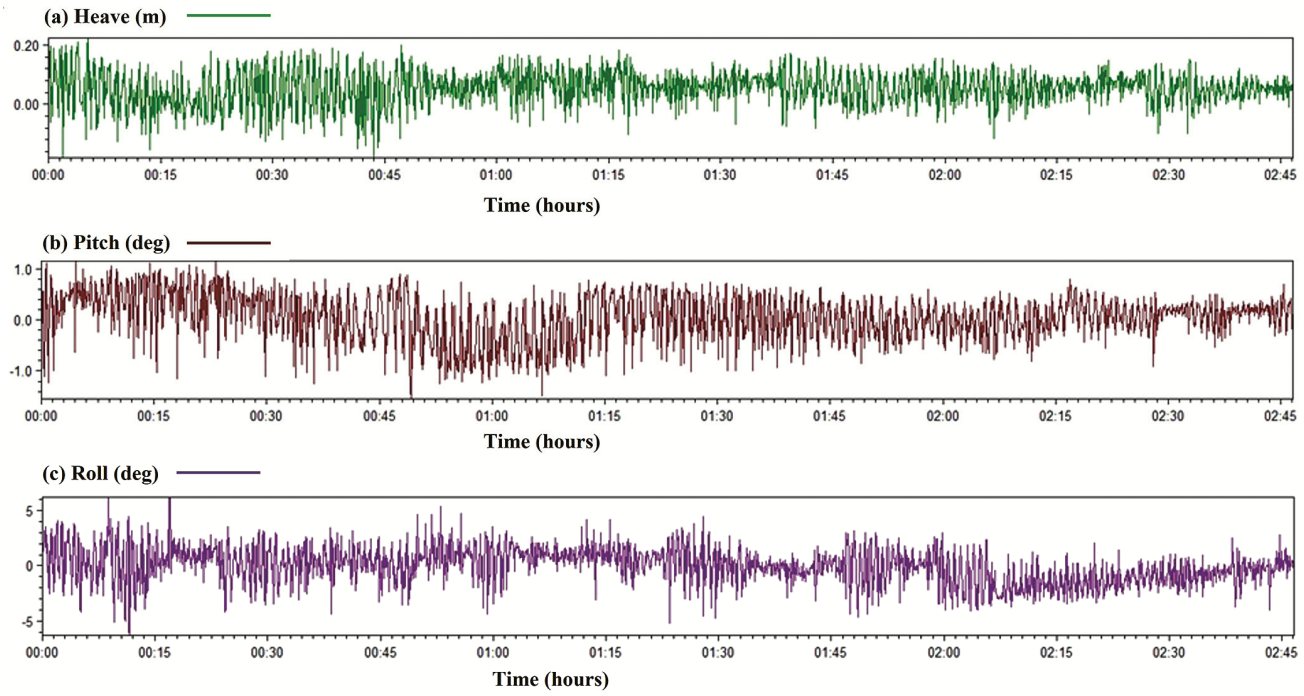

Fig. 6 — The measured heave (m), pitch (degree), and roll (degree) while varying the wave period from 1.22 to 2.13 s

resistance. The heaving buoy oscillates only in the vertical direction due to the wave force incident on it. The maximum and minimum wave power based on the theoretical formula is 23.19 W and 5.08 W, respectively. The wave force generated in the wave flume with the varied shutter frequency was in between 0.41 and 0.50 N/m.

The heave, pitch and roll of the buoy during the experiment in the wave flume were studied. Figure 6 shows that the variation of the pitch which is within -1° to +1° which is very less when compared to the changes along the heave. There are significant changes along the roll axis too. The heave, pitch and roll motion of the buoy gradually decreases while decreasing the shutter frequency from 60 to 35 Hz. The heave motion decreases approximately around ~0.35 m to 0.08 m by decreasing the wave frequency.

The wave generated acceleration by the sensor is monitored and measured for different wave conditions by varying the shutter frequency. The trends of the acceleration in X, Y & Z axes with varied wave frequency are presented in Figure 7. The measurement shows that the acceleration amplitudes reduce with respect to the decreasing wave action frequency. The acceleration in the three degrees of freedom with respect to X, Y & Z-axis are in the ranges -1 to 1 for X, -1 to 0.9 for Y, and -7.7 to -1.3 for Z axis.

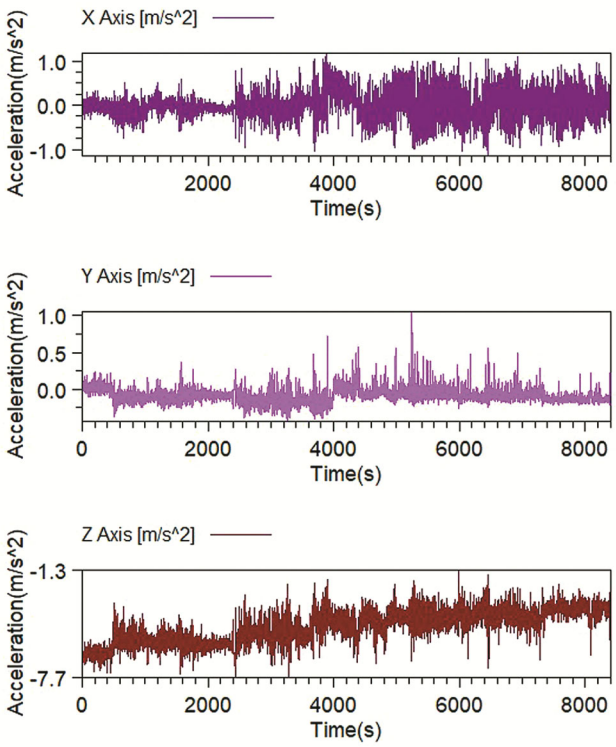

Fig. 7 — Measured acceleration (m/s^2) in X, Y & Z-axis for the varying wave period from 1.22 to 2.13 s

The voltage response under different excitation frequencies in the wave flume was studied. The shutter frequency was gradually deceased from 60 to

35 Hz by the regular interval of 5 Hz. The decrease in shutter frequency gradually decreases the wave height from ~0.21 to 0.06 m but it increases the wave period from 1.22 to 2.13 seconds. The voltage generated in the PEH system with the variable shutter frequency is shown in Figure 8. It can be seen that the voltage decreases with respect to wave shutter frequency. For a resistance of 10 kΩ, the generated voltage increases linearly with respect to the increasing shutter frequency.

The PEH harvester produces the maximum power at the resonance frequency which is 60 Hz. Table 1 shows the maximum voltage generated at each frequency along with the wave height and wave period. It is observed that a maximum of 2.56 V is generated for the frequency of 60 Hz and a minimum of 2.45 V is generated for the frequency of 30 Hz.

The generated voltage and power relationship were studied and the results show that the dynamic increase in wave conditions increases the vibration of the sensor thereby increasing the power and voltage output to maximum. The PEH setup in the present study makes use of 4 piezoelectric sensors and a floating buoy of 0.4 m diameter, buoyance weight 9.3 kg. Up scaling the size of buoy to 0.9 m diameter with more number of piezo sensors gives better voltage output. The Figure 8 shows that the increase in the voltage and power is due to the increase in wave period from 1.22 to 2.13 s.

The Figure 8 shows the graphical relationship of voltage and power generated in terms of shutter frequency. The voltage and power linearly increase with increasing wave forces. Figure 9 show the generated voltage due to the change of buoy acceleration in terms of wave flume shutter frequency and Figure 10 represents the voltage and power in terms of wave conditions. The experimental results are compared with the real wave conditions in the Lakshadweep Sea and near to Lakshadweep Island clusters where the wave parameter such as wave height, wave period and direction drastically changes during different monsoon seasons[23]. During the

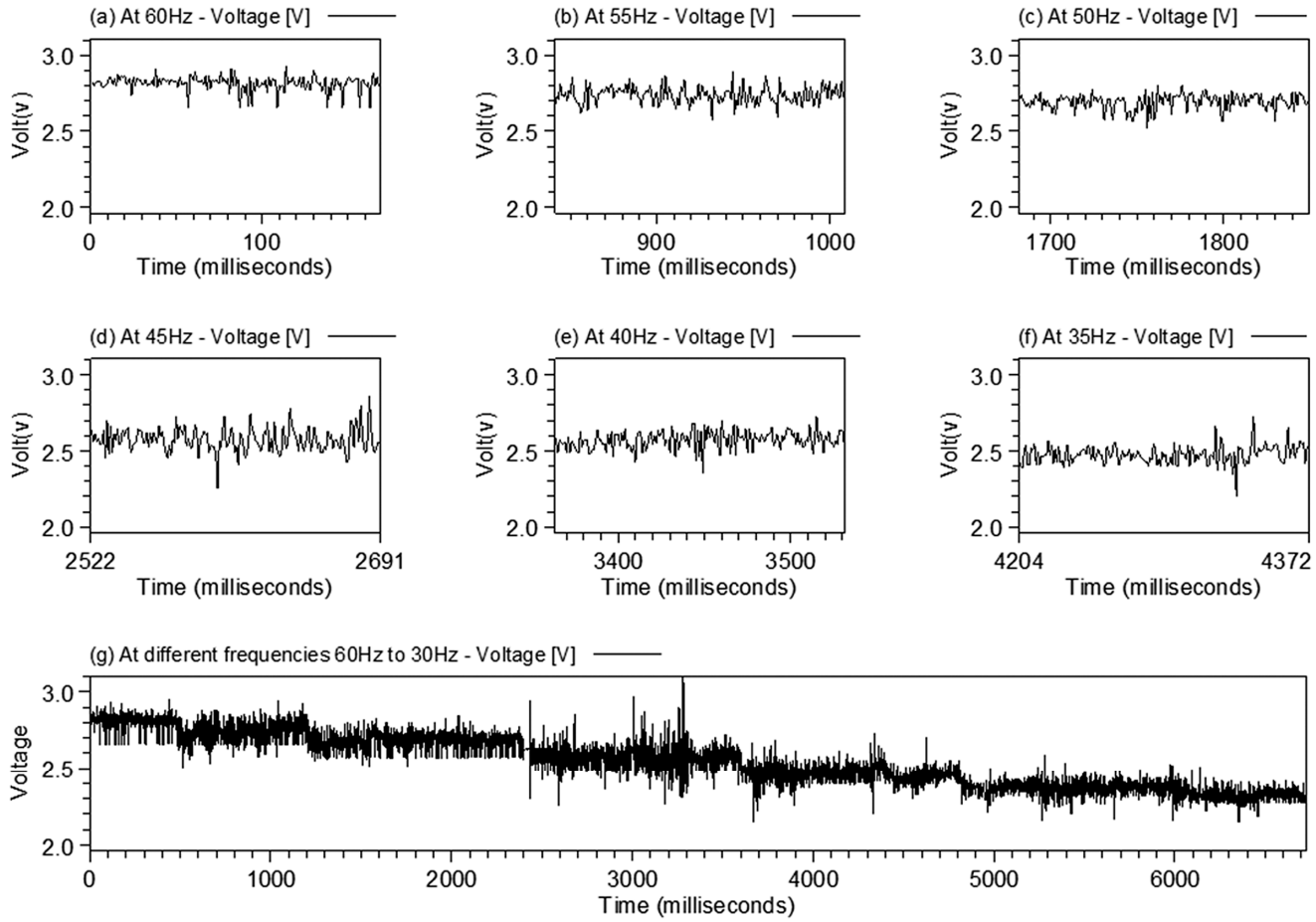

Fig. 8 — Generated voltage with respect to the changing wave period from 1.22 to 2.13 s

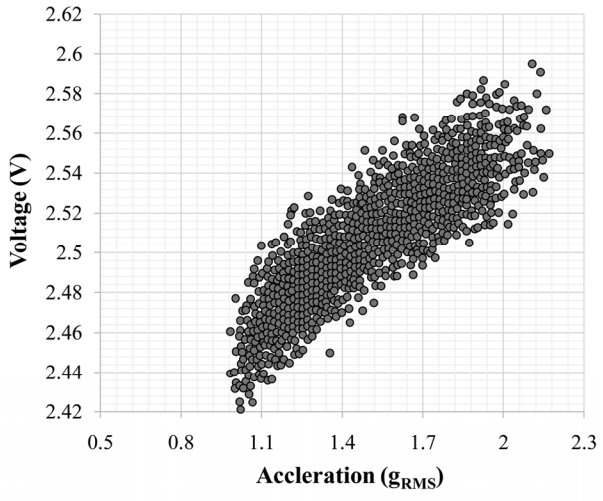

Fig. 9 — Generated voltage due to the change of buoy acceleration in terms of wave flume shutter frequency

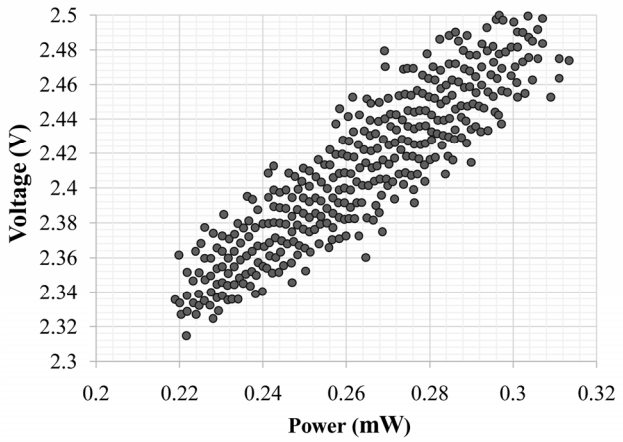

Fig. 10 — Generated voltage and power in terms of the wave conditions with the changing shutter frequency from 60 Hz to 35 Hz

southwest monsoon from June to August, the maximum significant wave height is around 1.5 to 2.4 m near to outer reef of lagoon area and around 3.5 m swell waves in-between the Island groups[23,24]. The wave period of the Lakshadweep Sea is in-between 4.8 to 14 s with an average of 8 s which implies that the wave power per unit area would be around 24 to 48 kW. Adopting the same PEH power generation technique for the higher wave period and 28 numbers of piezo diaphragms connected in 4×7 series/parallel connection a peak voltage of up to 16 V and power of 300 mW can be harnessed by regulating the current through the load resistance of 10 KΩ. Increasing the number of piezo sensors would increase the net output voltage and power compared to increasing the sizes of the piezo diaphragm. The real-time environment (open sea) exhibits irregular wave activity and the acceleration of the buoy varies with the irregular wave activity. The efficient bridge rectifier circuit and voltage regulator will regulate the AC voltage and power. The bridge rectifier and voltage regulator used in this system regulates voltage maximum up to 24 V. This harvesting technique will be very much useful for coastal and offshore buoys to harvest power in a hybrid approach during the failure in solar battery charging during monsoon and unfavorable weathers. Considering the limitations, regular maintenance of piezo sensor setup is required and the system will generate very less voltage if deployed in a very calm environment.

Conclusion

The concept of coupling the piezoelectric diaphragms to super balls increases the output of the piezo diaphragms by four times due to resonant vibration and wave acceleration. A maximum power of 0.31 mW is generated for the wave power of 23.19 W at the frequency of 60 Hz across 10 kΩ resistance using four piezoelectric diaphragms in the heaving buoy. If the number of piezo sensor diaphragms is increased to 28 and efficient materials are used to fabricate the diaphragms, then the output also would proportionally increase up to 16 V. These experimental results specify that the PEH system has a competence of low power generation with a range of 10 to 20 mW and it would be enhanced up to 300 mW by a force of a higher excitation frequency. Integration of the harvester setup inside the ocean physical and met-oceanic buoy makes it a cost-effective hybrid design; thereby making the setup viable for powering up the onboard sensors for remote oceanic applications.

Acknowledgements

This research did not receive any specific grant from funding agencies in the public, commercial, or not-for-profit sectors.

Conflict of Interest

The authors declare that they have no conflict of interest.

Ethical Statement

This research study is the authors' own original work, which has not been previously published elsewhere. This paper is not currently being

considered for publication elsewhere. The results are appropriately placed in the context of prior and existing research. All authors have been personally and actively involved in this extensive research work.

Author Contributions

JMH: Conceptualization, data curation, formal analysis, and writing - original draft. BVM: Conceptualization, Data curation, Formal analysis, Writing - review and editing. TPSJ: Conceptualization, Data curation, Writing - original draft.

References

1 Zhao T, Xu M, Xiao X, Ma Y, Li Z, *et al.*, Recent progress in blue energy harvesting for powering distributed sensors in ocean, *Nano Energy*, 88 (2021) p. 106199. https://doi.org/10.1016/j.nanoen.2021.106199

2 Masoumi M & Wang Y, Repulsive magnetic levitation-based ocean wave energy harvester with variable resonance: Modeling, simulation and experiment, *J Sound Vib*, 381 (2016) 192-205. https://doi.org/10.1016/ j.jsv.2016.06.024

3 Li Z, Peng Y, Xu Z, Peng J, Xin L, *et al*., Harnessing energy from suspension systems of oceanic vehicles with high-performance piezoelectric generators, *Energy*, 228 (2021) p. 120523. https://doi.org/10.1016/j.energy.2021.120523

4 Azam A, Ahmed A, Li H, Tairab A M, Jia C, *et al*., Design and analysis of the optimal spinning top-shaped buoy for wave energy harvesting in low energy density seas for sustainable marine aquaculture, *Ocean Eng*, 255 (2022) p. 111434. https://doi.org/10.1016/j.oceaneng.2022.111434

5 Grevemeyer I, Herber R & Essen H H, Microseismological evidence for a changing wave climate in the northeast Atlantic Ocean, *Nature*, 408 (6810) (2000) 349-352. https://doi.org/10.1038/35042558

6 Chang T, Wang Z, Yang Y, Luo Z, Wu C, *et al*., A case study on fiber optic interferometric seafloor seismic and Tsunami monitoring system in south China sea, *IEEE Trans Instrum Meas*, 70 (2020) 1-12. https://doi.org/10.1109/ TIM.2020.3017859

7 Li Y, Guo Q, Huang M, Ma X, Chen Z, *et al*., Study of an electromagnetic ocean wave energy harvester driven by an efficient swing body toward the self-powered ocean buoy application, *IEEE Access*, 7 (2019) 129758-129769. https://doi.org/10.1109/ACCESS.2019.2937587

8 Purser A & Thomsen L, Monitoring strategies for drill cutting discharge in the vicinity of cold-water coral ecosystems, *Mar Pollut Bull*, 64 (11) (2012) 2309-2316. https://doi.org/10.1016/j.marpolbul.2012.08.003

9 Xi F, Pang Y, Liu G, Wang S, Li W, *et al*., Self-powered intelligent buoy system by water wave energy for sustainable and autonomous wireless sensing and data transmission, *Nano Energy*, 61 (2019) 1-9. https://doi.org/10.1016/ j.nanoen.2019. 04.026

10 Wang Z L & Song J, Piezoelectric nanogenerators based on zinc oxide nanowire arrays, *Science*, 312 (5771) (2006) 242-246. https://doi.org/10.1126/science.1124005

11 Czech B & Bauer P, Wave energy converter concepts: design challenges and classification, *IEEE Ind Electron Mag*, 6 (2012) 4–16. https://doi.org/10.1109/MIE.2012.2193290

12 Falnes J, A review of wave-energy extraction, *Mar Struct*, 20 (4) (2007) 185-201. https://doi.org/10.1109/ MIE.2012. 2193290

13 Paakkinen H, Wave power plant, *US Patent no*. US8915077 B2 December 23, 2014. https://patents.google.com/ patent/ US8277146B2/en

14 Taylor G W, Burns J R, Kammann S A, Powers W B & Welsh T R, The energy harvesting eel: a small subsurface ocean/river power generator, *IEEE J Ocean Eng*, 26 (4) (2001) 539-547. https://doi.org/10.1109/48.972090

15 Li Z, Saadatnia Z, Yang Z & Naguib H, A hybrid piezoelectric-triboelectric generator for low-frequency and broad-bandwidth energy harvesting, *Energy Conv Manag*, 174 (2018) 188-197. https://doi.org/10.1016/j.enconman. 2018.08.018

16 Manbachi A & Cobbold R S, Development and application of piezoelectric materials for ultrasound generation and detection, *Ultrasound*, 19 (4) (2011) 187-196. https://doi.org/10.1258/ult.2011.011027

17 Wang W, Yang T, Chen X & Yao X, Vibration energy harvesting using a piezoelectric circular diaphragm array, *IEEE Trans Ultrason Ferroelectr Freq Control*, 59 (9) (2012) 2022-2026. https://doi.org/10.1109/TUFFC. 2012. 2422

18 Cross R, Impact behavior of a superball, *Am J Phys*, 83 (3) (2015) 238-248. https://doi.org/10.1119/1.4898312

19 Garwin R L, Kinematics of an ultraelastic rough ball, *Am J Phys*, 37 (1) (1969) 88-92. https://doi.org/10.1119/1.1975420

20 Dean R G & Dalrymple R A, *Water wave mechanics for engineers and scientists*, Vol 2, (World scientific publishing company), 1991, pp. 55-65.

21 Kamphuis J W, *Introduction to coastal engineering and management*, Vol 48, (World scientific publishing company), 2020, pp. 32-36.

22 Holthuijsen, L H, *Waves in oceanic and coastal waters*, (Cambridge university press), 2010 pp. 131-135.

23 Jinoj T P S, Bonthu S R, Robin R S, Idress Babu K K, Purvaja R, *et al*., Nearshore sediment dynamics of Kavaratti Island, Lakshadweep archipelago using integrated modelling system, *Indian J Geo-Mar Sci*, 49 (05) (2020) 845–857. https://nopr.niscpr.res.in/bitstream/123456789/54723/1/IJMS %2049(5)%20845-857.pdf

24 Prakash T N, Nair L S & Varghese T I, Shoreline changes and reef strengthening at Kavaratti island in Lakshadweep Archipelago-A case study, *Indian J Geo-Mar Sci*, 43 (07) (2014) 1140–1144. http://nopr.niscpr.res.in/handle/12345 6789/ =34418